Quarkyonic matter in lattice QCD at strong coupling

Kohtaroh MIURA[1], Takashi Z. NAKANO[2] and Akira OHNISHI[1]

[1] *Yukawa Institute of Theoretical Physics, Kyoto University, Kyoto 606-8502, Japan*
[2] *Department of Physics, Kyoto University, Sakyo-ku, Kyoto 606-8502*

We study the phase diagram of quark matter at finite temperature and density in the strong coupling lattice QCD with one species of unrooted staggered fermions including finite coupling ($1/g^2$) effects for color SU(N_c). We find that we may have partially chiral restored medium density matter at $N_c = 3$, which would correspond to the quarkyonic matter suggested at large N_c.

The QCD phase transition at finite temperature (T) is the latest vacuum phase transition in our universe, and it can be experimentally investigated at RHIC and LHC. Phase transitions at finite chemical potential (μ) in dense matter may be also realized during black hole formation or in neutron stars, where we have the following central question. *"What is the next to the hadronic Nambu-Goldstone phase in the larger μ direction ?"* Monte-Carlo (MC) simulations are not yet reliable in the region $\mu/T > 1$ because of the notorious sign problem, then it is necessary to invoke some approximations such as the large number of colors (N_c)[1)] or the strong coupling limit (SCL)[2)–9)] in order to answer this question in QCD.

Recently, McLerran and Pisarski have shown that the *next* phase at large N_c should be the so called *quarkyonic* phase, in which the colors are confined and the baryon density is high.[1)] At large N_c, gluon contribution to the pressure $\sim \mathcal{O}(N_c^2)$ is larger than those from hadrons $\sim \mathcal{O}(1)$ and quarks $\sim \mathcal{O}(N_c)$, then the deconfinement transition temperature T_d is independent of the quark chemical potential μ as far as it is moderate $\mu \sim \mathcal{O}(1)$. In the confined region $T < T_d$, quark number density is exponentially suppressed if μ is below the quark mass $m_q \sim \mathcal{O}(1)$, but it rapidly grows at $\mu > m_q$ and soon reaches high density $\sim \mathcal{O}(N_c)$. This dense matter has a characteristic feature that it is made of *quark*s, while only bar*yonic* excitations are allowed because it is confined. If the quarkyonic phase is the *next* at $N_c = 3$, it may be formed at high densities in compact astrophysical phenomena or in heavy-ion collisions at 10-100 A GeV. MC results with the density of state method also show the transition to high density phase,[10)] but its nature is not yet known. Very recently, quarkyonic matter is found to exist at $N_c = 3$ in effective models of QCD.[12)–14)] It is now very important and urgently required to discuss the possibility of the quarkyonic matter phase in QCD for $N_c = 3$.

The above discussion tells us that the quarkyonic transition, the transition from the chiral broken Nambu-Goldstone (NG) phase to the quarkyonic matter, is characterized by the quark number density. If the quarkyonic matter exists, the quarkyonic transition occurs at $\mu \sim m_q$ where density rapidly grows as $\rho_q = \mathcal{O}(1) \to \mathcal{O}(N_c)$, and the chiral restoration follows at higher chemical potential as shown in Fig. 1. In this paper, we discuss the possibility of the quarkyonic matter in the strong coupling lattice QCD (SC-LQCD),[2)–8)] which is another powerful tool in studying dense mat-

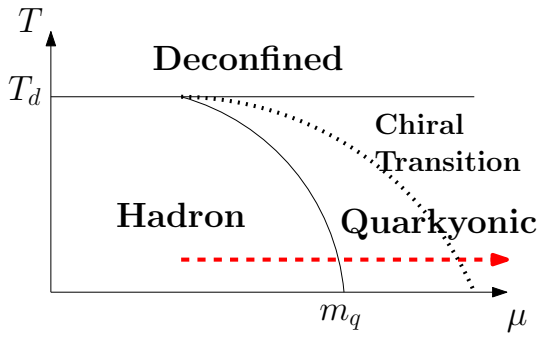

Fig. 1. Schematic phase diagram with the quarkyonic matter.

ter. We take account of the finite coupling effects in the next-to-leading order (NLO, $1/g^2$) ,[5)–8)] and introduce an auxiliary field representing the quark number density ρ_q as an order parameter in addition to the chiral condensate σ. In a previous work on the phase diagram with NLO effects,[7)] the order parameter representing ρ_q was not introduced. As shown later, the multi-order parameter (σ and ρ_q) treatment is essential in understanding the quarkyonic transition. In SC-LQCD, we consider the situation where g^2 is large while N_c is fixed. This condition is somewhat different from that assumed in the large N_c argument, where N_c is assumed to be large and the 't Hooft coupling $N_c g^2$ is fixed. As we show later, we find the quarkyonic matter to appear in some region of $1/g^2$ at $N_c = 3$. This observation together with the large N_c discussion[1)] support the existence of the quarkyonic matter in a wide region of the $(N_c, 1/g^2)$ plane.

We start from the lattice action with one species (unrooted, four flavors) of staggered fermions (χ) in the lattice unit,

$$S_{\rm LQCD} = \frac{1}{2}\sum_x \left[V^+(\mu) - V^-(\mu)\right] + \sum_x m_0 M_x + S^{(s)} - \frac{1}{g^2}\sum_{\square} {\rm tr}\left[U_{\square} + U_{\square}^\dagger\right] \ , \quad (1)$$

where m_0 and μ are the bare quark mass and the lattice chemical potential, respectively. The mesonic composites are defined as $M_x = \bar\chi_x \chi_x$, $V_x^+ = e^{\mu}\bar\chi_x U_{0,x}\chi_{x+\hat 0}$ and $V_x^- = e^{-\mu}\bar\chi_{x+\hat 0} U_{0,x}^\dagger \chi_x$, where sum over color indices are assumed. The spatial hopping action of quarks $S^{(s)}$ is given as,

$$S^{(s)} = \frac{1}{2}\sum_x \sum_{j=1}^{d} \eta_{j,x}\left[\bar\chi_x U_{j,x}\chi_{x+\hat j} - \bar\chi_{x+\hat j} U_{j,x}^\dagger \chi_x\right] \ , \quad (2)$$

where d is the spatial dimension and $\eta_{j,x} = (-1)^{x_0+\cdots+x_{j-1}}$ is the staggered sign factor. The gluon degrees of freedom are described by the temporal and spatial link variables and plaquettes, U_0, U_j, $U_{\square}$. This lattice action is invariant under the chiral transformation $\chi \to e^{i\theta\epsilon_x}\chi$ with the γ_5-related factor $\epsilon_x = (-1)^{x_0+\cdots+x_d}$.

In the strong coupling region ($g \gg 1$), we can evaluate the plaquette effects through the expansion in the power series of $1/g^2$ (strong coupling expansion). In each order of $1/g^2$ or the number of plaquette, we can exactly carry out the integral

over link variables by using the SU(N_c) group integral formulae, $\int dU\ U_{ab}U^{\dagger}_{cd} = \delta_{ad}\delta_{bc}/N_c$ and so on, and obtain the effective action of hadronic composites.[2)]

Before discussing the NLO effects, we briefly summarize the procedure to obtain the effective potential in the leading order, i.e. the strong coupling limit (SCL), where the sophisticated framework based on the $1/d$ expansion,[11)] mean field approximation and finite T treatments of the quark determinant,[3),6)] has been established. After the spatial link (U_j) integral, we obtain the hadronic hopping action shown in the third graph in Fig. 2[2)] from the spatial quark action $S^{(s)}$. The SCL effective action is given as,

$$S_{\rm SCL} = \frac{1}{2}\sum_x \left[V^+(\mu) - V^-(\mu)\right] + \sum_x m_0 M_x - \frac{b_\sigma}{2d}\sum_{x,j>0} M_x M_{x+\hat{j}} + \mathcal{O}\Big(\frac{1}{\sqrt{d}}, \frac{1}{g^2}\Big)\ , \tag{3}$$

where $b_\sigma = d/2N_c$. In this work, we adopt the leading order terms of the $1/d$ expansion[11)] and omit higher order terms $\mathcal{O}(1/\sqrt{d})$. In the $1/d$ expansion, the leading term $\sum_j M_x M_{x+\hat{j}}$ is assumed to remain finite at large d, then the quark fields scale as $\chi, \bar{\chi} \propto d^{-1/4}$ and higher power terms of quarks are found to be suppressed as $\mathcal{O}(1/\sqrt{d})$ for $N_c \geq 3$. Through the Hubbard-Stratonovich (HS) transformation, the chirally invariant four-fermi term $S_{\rm SCL}$ is converted to the quark mass term $b_\sigma\sigma\bar{\chi}\chi$, where the finite chiral condensate $\sigma = -\langle M_x\rangle$ breaks the chiral symmetry spontaneously and generates the quark mass dynamically. We can carry out the Gauss integral over the quark fields χ and $\bar{\chi}$ in the so-called finite temperature treatment: The determinant of the temporal quark hopping matrix with the anti-periodic boundary condition is obtained by utilizing the Matsubara product technique[3)] or the recursion relation.[6)] It is possible to carry out the temporal link integral of this determinant over U_0 in the Polyakov[3)] or temporal gauge.[6)] Then the effective potential is obtained as,

$$\mathcal{F}^{\rm SCL}_{\rm eff} = \frac{b_\sigma}{2}\sigma^2 + \mathcal{V}_q(m_q;\mu,T)\ , \tag{4}$$

$$\mathcal{V}_q(m_q;\mu,T) = -T\log\left[X_{N_c} + 2\cosh\Big[\frac{N_c\mu}{T}\Big]\right]\ , \tag{5}$$

$$X_{N_c}(m_q) = \frac{\sinh[(N_c+1)E_q(m_q)/T]}{\sinh[E_q(m_q)/T]}\ , \tag{6}$$

where we have regarded the inverse of the temporal extension $1/N_\tau$ as temperature T, and $E_q(m_q) = \mathrm{arcsinh}\,(m_q)$ represents the one dimensional quark excitation energy coming from the constituent quark mass $m_q = b_\sigma\sigma + m_0$.

We shall now evaluate NLO ($1/g^2$) correction terms coming from the plaquette action in $S_{\rm LQCD}$. We concentrate on the leading order of the $1/d$ expansion. By integrating out spatial link variables, two types of terms shown in the last two graphs in Fig. 2 are found to appear from temporal and spatial plaquettes,[5),6)]

$$\Delta S^{(\tau)}_\beta = \frac{\beta_\tau}{4d}\sum_{x,j>0}\left(V^+_x V^-_{x+\hat{j}} + V^+_x V^-_{x-\hat{j}}\right)\ , \tag{7}$$

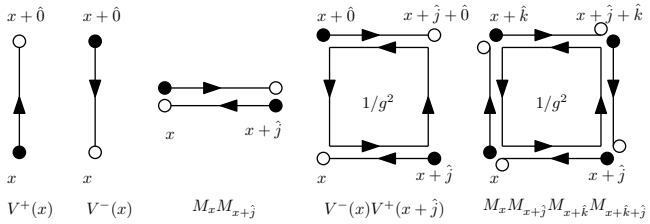

Fig. 2. Effective action terms in the strong coupling limit and NLO ($1/g^2$) corrections. Open circles, Filled circles, and arrows show χ, $\bar{\chi}$, and U_ν, respectively.

$$\Delta S_\beta^{(s)} = \frac{-\beta_s}{d(d-1)} \sum_{x,0<k<j} M_x M_{x+\hat{j}} M_{x+\hat{k}} M_{x+\hat{k}+\hat{j}} \ , \tag{8}$$

where $\beta_\tau = d/N_c^2 g^2$ and $\beta_s = d(d-1)/8N_c^4 g^2$.

The NLO terms contain the product of different types, such as V^+V^- in $\Delta S_\beta^{(\tau)}$. In order to treat these terms, we propose a new mean field technique, named Extended Hubbard-Stratonovich (EHS) transformation. Let us consider to evaluate a quantity $e^{\alpha AB}$, where (A, B) and α represent arbitrary composite fields and an positive constant, respectively. We can represent $e^{\alpha AB}$ in the form of Gaussian integral over two auxiliary fields (φ, ϕ),

$$\begin{aligned} e^{\alpha AB} &= \int d\varphi\, d\phi\, e^{-\alpha\left\{(\varphi-(A+B)/2)^2+(\phi-i(A-B)/2)^2\right\}+\alpha AB} \\ &= \int d\varphi\, d\phi\, e^{-\alpha\left\{\varphi^2-(A+B)\varphi+\phi^2-i(A-B)\phi\right\}} \ . \end{aligned} \tag{9}$$

The integral over the new fields (φ, ϕ) is approximated by the saddle point value, $\varphi = \langle A+B\rangle/2$ and $\phi = i\langle A-B\rangle/2$. Specifically in the case where both $\langle A\rangle$ and $\langle B\rangle$ are real, which applies to the later discussion, the stationary value of ϕ becomes pure imaginary. Thus we replace $\phi \to i\omega$ and require the stationary condition for the real value of ω,

$$e^{\alpha AB} \approx e^{-\alpha\left\{\varphi^2-(A+B)\varphi-\omega^2+(A-B)\omega\right\}}\Big|_{\text{stationary}} \ . \tag{10}$$

In the case of $A = B$, Eq. (10) reduces to the standard HS transformation. We find that the $e^{\alpha AB}$ is invariant under the scale transformation, $A \to \lambda A$ and $B \to \lambda^{-1}B$. This invariance is kept in rhs of Eq. (10), since the combinations $\varphi - \omega = \langle A\rangle$ and $\varphi + \omega = \langle B\rangle$ transform in the same way as A and B, respectively. This means that the effective potential is independent of the choice of λ.

We apply the EHS transformation to the NLO terms. For the temporal and spatial plaquette action terms, $\Delta S_\beta^{(\tau)}$ and $\Delta S_\beta^{(s)}$, we substitute $(\alpha, A, B) = (\beta_\tau/4d, -V_x^+, V_{x+\hat{j}}^-)$ and $(\beta_s/d(d-1), M_x M_{x+\hat{j}}, M_{x+\hat{k}} M_{x+\hat{k}+\hat{j}})$ in Eq. (10), respectively, and obtain,

$$\Delta S_\beta^{(\tau)} \approx \frac{\beta_\tau}{4d} \sum_{x,j>0} \left[\varphi_\tau^2 - \omega_\tau^2 + (\varphi_\tau - \omega_\tau)V_x^+(\mu) \ -(\varphi_\tau + \omega_\tau)V_x^-(\mu)\right] + (j \leftrightarrow -j) \ , \tag{11}$$

$$\Delta S_\beta^{(s)} \approx \frac{\beta_s}{d(d-1)} \sum_{x,0<k<j} \left[\varphi_s^2 - \omega_s^2 - (\varphi_s - \omega_s) M_x M_{x+\hat{j}} - (\varphi_s + \omega_s) M_{x+\hat{k}} M_{x+\hat{k}+\hat{j}}\right] . \tag{12}$$

We can absorb NLO terms, $\Delta S_\beta^{(\tau,s)}$ in Eqs. (11) and (12), in the coefficient modification of the SCL effective action, $S_{\rm SCL}$ in Eq. (3). We assume that auxiliary fields take constant and isotropic values, which are independent from the space-time x and spatial directions j, k. In $\Delta S_\beta^{(s)}$, effects of ω_s disappear for constant auxiliary fields, and φ_s modifies the coefficient of MM terms in $S_{\rm SCL}$ as $-b_\sigma/2d \to -\tilde{b}_\sigma/2d$, where $\tilde{b}_\sigma = b_\sigma + 2\beta_s\varphi_s$. Combined with the temporal hopping term in $S_{\rm LQCD}$, the coefficients of $V^\pm$ are found to be, $Z_\mp/2$, where $Z_\pm = 1 + \beta_\tau(\phi_\tau \pm \omega_\tau)$. We rewrite these coefficients as $Z_\pm = Z_\chi \exp(\pm\delta\mu)$, then NLO effective action containing fermions is written as,

$$S_{\rm NLO}^{(F)} = \frac{Z_\chi}{2} \sum_x \left[V^+(\tilde{\mu}) - V^-(\tilde{\mu})\right] + \sum_x m_0 M_x - \frac{\tilde{b}_\sigma}{2d} \sum_{x,j>0} M_x M_{x+\hat{j}} + \mathcal{O}\Big(\frac{1}{\sqrt{d}}, \frac{1}{g^2}\Big) , \tag{13}$$

where $\tilde{\mu} = \mu - \delta\mu = \mu - \log\sqrt{Z_+/Z_-}$ and $Z_\chi = \sqrt{Z_+ Z_-}$ represent shifted chemical potential and the wave function renormalization factor.

Now we can repeat the same procedure as the standard SCL prescription. Bosonization of the four-fermi interaction in $S_{\rm NLO}$ leads to the quark mass term $(\tilde{b}_\sigma\sigma + m_0)M$, and the quark integral and the temporal link integral are also analogous to the SCL case. The effects of wave functional renormalization factor Z_χ would be a little bit non-trivial: Let us define the temporal hopping matrix as $\sum_{xy} \bar{\chi}_x K^{(\tau)}_{xy} \chi_y \equiv \sum_x [V_x^+ - V_x^-]/2$, then the quark determinant in SCL reads $\mathrm{Det}\big[K^{(\tau)} + \mathbf{1}(b_\sigma\sigma + m_0)\big]$. With NLO effects, this determinant is replaced with,

$$\mathrm{Det}\Big[Z_\chi K^{(\tau)}(\tilde{\mu}) + \mathbf{1}(\tilde{b}_\sigma\sigma + m_0)\Big] = \mathrm{Det}\big[Z_\chi\big]\mathrm{Det}\Big[K^{(\tau)}(\tilde{\mu}) + \mathbf{1}(\tilde{b}_\sigma\sigma + m_0)/Z_\chi\Big] , \tag{14}$$

where Det represents the determinant of the temporal and the color matrix. From the factor $\mathrm{Det}\big[Z_\chi\big]$ in Eq. (14), the additional term $-N_c \log Z_\chi$ appears in the effective potential. The second factor in the second line of Eq. (14) leads to $\mathcal{V}_{\rm q}$ with modified quark mass and chemical potential. Note that the quark mass is also modified by Z_χ. Finally the effective potential is found to be,

$$\mathcal{F}_{\rm eff} = \mathcal{F}_{\rm aux} + \mathcal{V}_{\rm q}(\tilde{m}_q; \tilde{\mu}, T) , \tag{15}$$

$$\mathcal{F}_{\rm aux} = \frac{\tilde{b}_\sigma}{2}\sigma^2 + \frac{\beta_\tau}{2}(\varphi_\tau^2 - \omega_\tau^2) + \frac{\beta_s}{2}\varphi_s^2 - N_c \log Z_\chi , \tag{16}$$

$$\tilde{m}_q = (\tilde{b}_\sigma\sigma + m_0)/Z_\chi . \tag{17}$$

We find that the plaquette contributes to the effective potential in the modification of the wave function renormalization factor Z_χ, the quark mass $\tilde{m}_q$, and the shift of the effective potential $\tilde{\mu}$ in addition to some auxiliary field terms, $\mathcal{F}_{\rm aux}$.

Since the $1/g^4$ contributions have ambiguities in the present NLO treatment, we here compare the results in several ways of truncation. In the first treatment, abbreviated as NLO-A, $\mathcal{F}_{\rm eff}$ in Eq. (15) is treated as it is, and we do not invoke any further approximations. In the second treatment (NLO-B), $\mathcal{O}(1/g^4)$ contributions in Z_χ and $\tilde{\mu}$ are truncated, and simplified as $Z_\chi = 1 + \beta_\tau \varphi_\tau$ and $\tilde{\mu} = \mu - \beta_\tau \omega_\tau$. In this treatment, we find that φ_τ and ω_τ couple to quarks separately through $\tilde{m}_q$ and $\tilde{\mu}$ in $\mathcal{V}_{\rm q}$, respectively. In the third prescription (NLO-C), we further truncate $\mathcal{O}(1/g^4)$ terms in $\tilde{m}_q$ and in $\log Z_\chi$. It is also possible to expand $\mathcal{V}_{\rm q}$ with respect to $\delta\mu = \mu - \tilde{\mu}$ (NLO-D),

$$\mathcal{V}_{\rm q}(\tilde{m}_q; \tilde{\mu}, T) \simeq \mathcal{V}_{\rm q}(\tilde{m}_q; \mu, T) - \beta_\tau \omega_\tau \partial \mathcal{V}_{\rm q}/\partial\mu \ . \tag{18}$$

In each treatment NLO-A,B,C, and D, we evaluate $\mathcal{F}_{\rm eff}$ under the stationary condition with respect to the auxiliary fields, $\Phi = \sigma, \varphi_s, \varphi_\tau, \omega_\tau$,

$$\frac{\partial \mathcal{F}_{\rm eff}}{\partial \Phi} = \frac{\partial \mathcal{F}_{\rm aux}}{\partial \Phi} + \frac{\partial \mathcal{V}_{\rm q}}{\partial \tilde{m}_q}\frac{\partial \tilde{m}_q}{\partial \Phi} + \frac{\partial \mathcal{V}_{\rm q}}{\partial \tilde{\mu}}\frac{\partial \tilde{\mu}}{\partial \Phi} = 0 \ . \tag{19}$$

Note that $\mathcal{V}_{\rm q}$ depends on the auxiliary fields via the two dynamical variables $\tilde{m}_q$ and $\tilde{\mu}$. Here we show the stationary conditions in NLO-A, as an example. Substituting σ for Φ in Eq. (19), we obtain the relation, $\sigma = -(1/Z_\chi)(\partial \mathcal{V}_{\rm q}/\partial m_q)$. By utilizing this result, the stationary condition for φ_s leads to $\varphi_s = \sigma^2$. We can solve the coupled equation for the stationary conditions of φ_τ and ω_τ as,

$$\varphi_\tau = \frac{2\varphi_0}{1 + \sqrt{1 + 4\beta_\tau \varphi_0}} \ , \qquad \omega_\tau = -\frac{\partial \mathcal{V}_{\rm q}}{\partial \tilde{\mu}} \equiv \rho_q \ , \tag{20}$$

where $\varphi_0 = N_c - Z_\chi \tilde{m}_q + \beta_\tau \omega_\tau^2$. The second equation in Eq. (20) indicates the auxiliary field ω_τ is nothing but the quark number density ρ_q. The equilibrium condition is determined self-consistently by minimizing $\mathcal{F}_{\rm eff}$ in terms of σ under the constraint $\omega_\tau = \rho_q(T, \mu; \sigma, \omega_\tau)$. Stationary conditions in NLO-B, C and D are solved similarly. In NLO-D, ω_τ is explicitly obtained as a function of σ, $\omega_\tau = -\partial \mathcal{V}_{\rm q}(m_q(\sigma); \mu, T)/\partial\mu$, where the rhs does not contain ω_τ. In this meaning, the NLO-D gives a similar formulation to that in the previous work.[7)]

One of the most interesting features in the multi-order parameter treatments (NLO-A, B and C) is that it predicts the existence of partially chiral restored (PCR) matter at $N_c = 3$ for relatively large $\beta = 6/g^2$ values. In Fig. 3, we show the phase diagram at $\beta = 4.5$ in the chiral limit. In NLO-A and B, the highest temperature of the first order phase boundary decreases, and the critical point deviates from the second order phase transition boundary at $6/g^2 \simeq 4.5$ and 3.0 in NLO-A and NLO-B, respectively. In NLO-C, the second order critical chemical potential $\mu_c^{(2nd)}$ at $T = 0$ overtakes the first order one at $6/g^2 \simeq 3.5$. Between the first and second order phase boundaries, we find PCR matter.

In Fig. 4, we show the comparison of ρ_q and σ in the present treatments NLO-A, B, C and D. The gradual increase of the quark density is a common feature of the multi-order parameter treatments. At low temperatures, we can investigate the appearance of the medium density matter more intuitively. The quark number

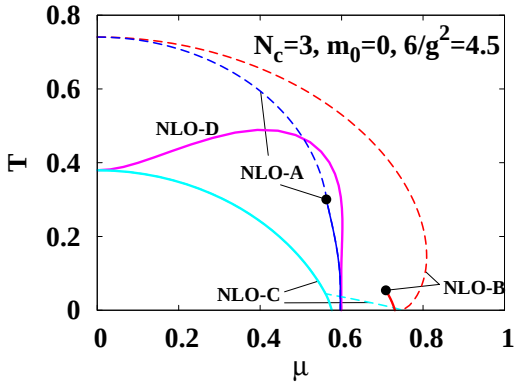

Fig. 3. Phase diagram in NLO-A, B, C and D with $N_c = 3, 6/g^2 = 4.5$ Solid and dashed lines show the first and second order phase transition boundary, respectively.

density $\rho_q = -\partial \mathcal{F}_{\rm eff}/\partial\mu$ is evaluated as,

$$\frac{\rho_q}{N_c} = \frac{2\sinh\left[N_c\tilde{\mu}/T\right]}{X_{N_c} + 2\cosh\left[N_c\tilde{\mu}/T\right]} \underset{T\to 0}{\longrightarrow} \frac{x^{N_c}}{1+x^{N_c}}\ , \tag{21}$$

where $x = \exp[-(E_q - \tilde{\mu})/T]$. When $E_q > \tilde{\mu}$ is satisfied at small T, we obtain $x \to 0$ and $\rho_q \to 0$, while $E_q < \tilde{\mu}$ leads to $x \to \infty$ and $\rho_q \to N_c$. Medium density $0 < \rho_q < N_c$ can appear only in the case where the energy and chemical potential balances, $E_q = \tilde{\mu}$, and x stays finite at $T = 0$. Since $\tilde{\mu}$ is a decreasing function of ω_τ, we may have a medium density solution of Eq. (20) in the region $\tilde{\mu}(\sigma, \omega_\tau = N_c) < E_q(\sigma, \omega_\tau) < \mu$. Specifically in NLO-B and C, $E_q = \tilde{\mu}$ is found to be equivalent to the density condition $\rho_q = (\mu - E_q)/\beta_\tau$, which can take the a medium value. In the large β region, this medium density matter can emerge in equilibrium as indicated in Fig. 4. Also in NLO-A, medium density matter appears in a similar mechanism. Thus the multi-order parameter treatment is essential to obtain the medium density matter at low T, and we observe chiral transitions twice as μ increases. After the first one, the condition $E_q = \tilde{\mu}$ is approximately satisfied. This state may correspond to the quarkyonic matter where we expect $\mu \sim$(constituent quark mass).[14)]

In summary, we have evaluated the effective potential in the next-to-leading order strong coupling lattice QCD (NLO SC-LQCD), where $1/g^2$ effects are taken into account. We have discussed the chiral transition and the possibility of the quarkyonic transition. Here the order parameter of the latter is the quark number density, which can be naturally introduced via the NLO effects. The $\mathcal{O}(1/g^4)$ ambiguities have been examined by comparing the results in several truncation schemes, and we have found the following common properties as far as the quark number density is treated as the order parameter in addition to the chiral condensate. (I) The partially chiral restored (PCR) matter can appear in the large $6/g^2$ region, (II) PCR sits next to the hadronic Nambu-Goldstone (NG) phase in the μ direction, (III) the quark number density is high as $\mathcal{O}(N_c)$ in PCR, (IV) after the "NG→PCR transition", the effective chemical potential is approximately the same as the quark excitation energy, (V) and the chiral transition to the Wigner phase follows after NG→PCR

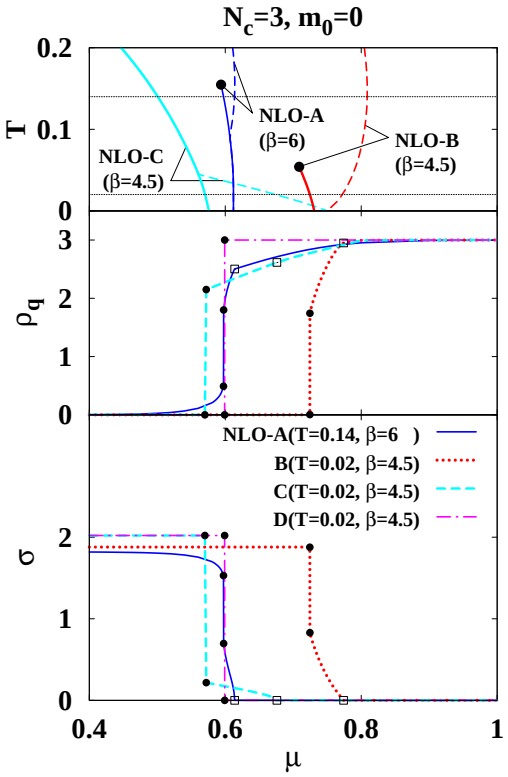

Fig. 4. In the upper panel, solid and dashed curves show the first and second order phase transition boundaries, and dots show the critical end point. In the middle and lower panels, solid, dotted, dashed, and dot-dashed curves show the results in NLO-A, B, C and D, respectively, and dots and open squares show the first and second order transition points.

transition. All these properties would be the essence of the quarkyonic matter and transition proposed in Ref.[1] In the previous work, the quark-driven Polyakov loop evaluated in SC-LQCD is shown to be small as $\mathcal{O}(1/N_c)$,[6] and it would not grow much at low temperatures. This feature also agrees with the proposed property of the quarkyonic matter. In the present analyses, we have found the two sequential chiral transitions can occur along the μ direction at low T, and the first one involves the quarkyonic transition. Thus we can conclude that we have examined the quarkyonic picture with the clear connection to the finite coupling effects in the strong coupling expansion. The detailed analyses of the phase diagram evolution due to the finite coupling effects will be shown elsewhere.[16]

There are many points to be improved in the present analysis. First, $\mathcal{O}(1/g^4)$ ambiguities is not small, and it is necessary to extend the analysis to the next-to-next-to-leading order (NNLO). Higher orders in $1/d$ expansion may be also necessary. The quarkyonic transition may be related to the so-called baryon mass puzzle;[9),17)] $N_c\mu_c$ is calculated to be smaller than the baryon mass in the strong coupling limit. This means that the chiral transition takes place before nuclear matter is formed. The chemical potential shift discussed in this paper may be the key to solve this problem.

Competition with the color superconducting (CSC) phase and the inhomogeneous chiral density wave states,[18] and comparison with the MC results at finite baryon density[10),15] are other interesting subjects to be investigated.

This work has been motivated by the discussions during the international workshop on "New Frontiers in QCD 2008". We would like to thank Prof. Larry McLerran, Prof. Kenji Fukushima, and other participants in that workshop. We would like to thank Prof. Noboru Kawamoto and Prof. Philippe de Forcrand for useful discussions. This work was supported in part by the Grant-in-Aid for Scientific Research from MEXT and JSPS under the grant numbers, 17070002 and 19540252, the Global COE Program "The Next Generation of Physics, Spun from Universality and Emergence", and the Yukawa International Program for Quark-hadron Sciences (YIPQS).

---

1) L. McLerran and R. D. Pisarski, Nucl. Phys. A **796** (2007), 83; Y. Hidaka, L. D. McLerran and R. D. Pisarski, Nucl. Phys. A **808** (2008), 117.
2) N. Kawamoto and J. Smit, Nucl. Phys. B **192** (1981), 100; H. Kluberg-Stern, A. Morel, O. Napoly and B. Petersson, Nucl. Phys. B **190** (1981), 504; J. Hoek, N. Kawamoto and J. Smit, Nucl. Phys. B **199** (1982), 495; K. Fukushima, Prog. Theor. Phys. Suppl. **153** (2004), 204; Y. Nishida, Phys. Rev. D **69** (2004), 094501.
3) P. H. Damgaard, N. Kawamoto, K. Shigemoto, Phys. Rev. Lett. **53** (1984), 2211; Nucl. Phys. **B264** (1986), 1.
4) N. Kawamoto, K. Miura, A. Ohnishi, T. Ohnuma, Phys. Rev. D **75** (2007), 014502.
5) T. Jolicoeur, H. Kluberg-Stern, M. Lev, A. Morel and B. Petersson, Nucl. Phys. B **235** (1984), 455.
6) G. Faldt and B. Petersson, Nucl. Phys. B **265** (1986), 197.
7) N. Bilić, F. Karsch and K. Redlich, Phys. Rev. D **45** (1992), 3228. N. Bilić and J. Cleymans, Phys. Lett. B **355** (1995), 266.
8) A. Ohnishi, N. Kawamoto and K. Miura, J. Phys. G **34** (2007), S655; A. Ohnishi, N. Kawamoto, K. Miura, K. Tsubakihara and H. Maekawa, Prog. Theor. Phys. Suppl. **168** (2007), 261.
9) B. Bringoltz, JHEP **0703** (2007), 016; B. Bringoltz and B. Svetitsky, Phys. Rev. D **68** (2003), 034501.
10) Z. Fodor, S. D. Katz and C. Schmidt, JHEP **0703** (2007), 121.
11) M. E. Fisher and D. S. Gaunt, Phys. Rev. 1A **133** (1964), A244; H. Kluberg-Stern, A. Morel and B. Petersson, Nucl. Phys. B **215** (1983), 527.
12) L. Y. Glozman and R. F. Wagenbrunn, Phys. Rev. D **77** (2008), 054027.
13) K. Fukushima, Phys. Rev. D **77** (2008), 114028; H. Abuki, R. Anglani, R. Gatto, G. Nardulli and M. Ruggieri, Phys. Rev. D **78** (2008), 034034.
14) L. McLerran, K. Redlich and C. Sasaki, arXiv:0812.3585.
15) M. D'Elia and M. P. Lombardo, Phys. Rev. D **67** (2003), 014505; P. de Forcrand and O. Philipsen, Nucl. Phys. B **673** (2003), 170; P. de Forcrand and S. Kim, Phys. Lett. B **645** (2007), 339; M. Fromm and P. de Forcrand, arXiv:0811.1931; P. de Forcrand and M. Fromm, arXiv:0907.1915.
16) K. Miura, T. Z. Nakano, A. Ohnishi and N. Kawamoto, arXiv:0907.4245 [hep-lat].
17) P. de Forcrand and S. Kim, Phys. Lett. B **645** (2007), 339; I. M. Barbour, S. E. Morrison, E. G. Klepfish, J. B. Kogut and M. P. Lombardo, Phys. Rev. D **56** (1997), 7063; K. Miura, A Ohnishi, N Kawamoto, PoS **LAT2008** (2008), 075.
18) E. Shuster and D. T. Son, Nucl. Phys. B **573** (2000) 434; B. Y. Park, M. Rho, A. Wirzba and I. Zahed, Phys. Rev. D **62** (2000) 034015; R. Rapp, E. V. Shuryak and I. Zahed, Phys. Rev. D **63** (2001) 034008; D. V. Deryagin, D. Y. Grigoriev and V. A. Rubakov, Int. J. Mod. Phys. A **7** (1992) 659; E. Nakano and T. Tatsumi, Phys. Rev. D **71** (2005) 114006.